Experiments in Fluids 23 (1997) 113–120

Direct measurements of in-cylinder integral length scales of a transparent engine

C. W. Hong, D. G. Chen

Abstract This paper presents a hardware technology and its accompanying software developed to measure the in-cylinder integral length scales of the flow inside a transparent four-stroke engine directly, using a fiber laser Doppler velocimeter (LDV). A traverse table was designed to combine two 1-component fiber optical probes to form an LDV system with the capability of both 2-component single- point and 1-component two-point simultaneous measurements for velocities. This paper demonstrates the evaluation of radially separated lateral and longitudinal integral length scales. The location was at a mid-plane of the top dead center (TDC) clearance height, and the engine was motored at a speed of 500 rpm. Data analysis was processed using statistical techniques and the physical meaning of the results was explained.

1 Introduction

The engine design has come to an advanced level that the in-cylinder fluid motion has to be optimized nowadays due to stringent emission laws. To refine the combustion system design, the flow process has to be carefully studied. The in-cylinder air motion is inherently a periodic nonstationary turbulent flow with cycle variation. Both modern techniques of computational fluid dynamics (CFD) and nonintrusive laser diagnostics can be employed to investigate the in-cylinder flow field qualitatively as well as quantitatively. However, poor CFD predictions may be resulted due to lack of suitable in-cylinder turbulence models. Part of the incentive of this research was to investigate the measurement of the detailed flow structure for future in-cylinder turbulence modelling. According to the fundamental turbulence physics, the major two parameters which represent the turbulent flow characteristics are the (temporal) turbulence intensity and the (spatial) integral length scales. The former is a measure of the characteristic speed of the turbulent flow over a characteristic distance; while the latter is a quantitative measure of the distance characteristic of the flow structure.

Received: *27 August 1996/Accepted*: *6 December 1996*

C. W. Hong, D. G. Chen
Department of Power Mechanical Engineering National Tsing Hua University, Hsinchu 30043, Taiwan

Correspondence to: C. W. Hong

Thanks are due to the National Science Council, R.O.C. for financial support under contract no. NSC-84-2212-E007-001.

An LDV system is the most common optical diagnostic instrument in internal combustion engine laboratories. To make the most of using such a system, the length scale measurement is a good extension to expand its usefulness, especially when dealing with the comparison of CFD simulation with experimental results. Substantial amounts of effort have been focused on the measurement of temporal characteristics of the in-cylinder fluid motion in the past. The initial length scale LDV measurement was related to the measurement of temporal time scales using traditional single-point method (example: Liou and Satavicca 1985, and many others). Unfortunately, the strong mean motion which is required from the relation does not exist in the nonstationary in-cylinder turbulent flow field. Hence, such kind of measurement can only be referred as a preliminary estimate of length scales; or termed as an "indirect measurement".

A "direct measurement" of length scales requires the simultaneous acquisition of at least two spatially separated velocity measurements. There have been only few attempts of direct measurements of the in-cylinder integral length scales using nonintrusive optical instruments. Various methods were reported in the literature, such as using laser homodyne principle (Ikegami et al. 1987), or a scanning LDV (Glover et al. 1988), or employing a elongated single-probe-volume two-point LDV (Fraser et al. 1986, 1988, 1989), or recently a modern two-probe-volume two-point LDV (Corcione and Valentino 1990). However, they all meet varying degree of difficulties and limitations. The laser homodyne principle detects the relative fluid motion in the measuring volume directly by finding the light-intensity fluctuation. The major disadvantage of this method is that large measuring volume length is required and isotropic turbulence has to be assumed throughout. Hence, it suffers from the resolution and accuracy problem. The rotating mirror mechanism of the scanning LDV is a very innovative device. It eliminates the cycle variation problem during measurement, but the mechanism and control devices are a bit too complex. The single-probe two-point LDV method uses a long focal length lens to focus two parallel laser beams into a long narrow probe volume on the intersection. The scattered light was collected from two distinct locations within the elongated probe volume. The device is very simple but the range of the measurement of length scales is limited by the length of the elongated volume, 5 mm according to the literature. The modern two-probe-volume two-point method uses two separated mirrors to manipulate the relative position of two focused points. The range is much wider (10 mm), but it causes some problems of optics alignment.

This paper introduces a very simple and cheap mechanism to extend a two-probe 2-component LDV system to be capable of two-point 1-component measurement of length scales as well. The relative position and direction of two-point measurements are more manipulatable than the previous device. This system does not have range limitation and is good at resolution if micrometers are used. Part of the objectives of this research was to provide further detailed structure of the turbulent flow within internal combustion engines, especially in-cylinder spatial characteristics. In addition, the results of this work also provide data for the assessment of in-cylinder turbulence modelling.

2 Test rig and experimental process

A single-cylinder four-stroke research engine with compression ratio of 4:1 was used. The specifications of this engine are displayed in Table 1. It has been modified to be optical accessible by replacing the liner with a quartz tube. The piston head was trimmed to be flat in order to simplify the shape of the combustion chamber to be pan-cake type. Three teflon piston rings were used to reduce the problem of optical window fouling and also in case of scuffing the quartz liner. The engine was operated under motoring condition without cylinder lubrication. An optical encoder, connected to the crank shaft, generates 720 pulses per revolution. The pulses were processed by a rotating machinery resolver to synchronize burst detectors in the signal processor. Figure 1 shows the schematic configuration of the engine, the dynamometer, the seeding generator, and the LDV system. Basically, the LDV has two fiber optical probes. The system comprises a 5 W argon-ion laser that utilizes the blue and purple beams (;green light was connected to another 1-component system during then). Compressed air was processed by a dryer before entering the seeding generator, which uses the reversed cyclone principle to scatter MgO particles to the air flow. A piezoelectric transducer located at the top of the cylinder head is for cylinder pressure measurements. This is to assure that the in-cylinder test conditions are repeatable. The detailed specifications of the

Table 1. Specifications of the research engine

Model	Megatech Mark III
No. of cylinder	1
No. of strokes	4
Bore	41 mm
Stroke	51 mm
Connecting rod length	165 mm
Displacement	68 c.c.
Compression ratio	4
Inlet valve open (IVO)	0° ATDC
Inlet valve closure (IVC)	28° ABDC
Exhaust valve open (EVO)	46° BBDC
Exhaust valve closure (EVC)	13° ATDC

LDV system are displayed in Table 2. The Doppler signal was processed by a digital burst correlator, TSI IFA 750. An IBM PC 486 was connected to process the large amount of data, and also to control the sequence of the test.

In order to convert the original 2-probe LDV system to be capable of both 2-component single-point measurement and 1-component two-point measurement of length scales, a traverse table was designed as shown in Fig. 2. The relative position of the two fiber probes can be adjusted from the X–Y translation and rotation stage. The focal lengths of transmitting lenses for the two fiber probes are different from each other. They are 500 mm for the blue lines, and 350 mm for the purple lines. The purpose is to avoid collision of the two fiber optic probes when the measurement points are too close to each other. For simultaneous two-point measurements, the location of the fixed point is at the center of the horizontal plane 13 mm below the flat cylinder head. The direction of moving the changeable point is along the radial direction of the plane or the X_1 and X_2 axes as shown in Fig. 3. They are termed as longitudinal and lateral length scales, which will be explained in the third section.

From preliminary tests, the data sampling rate of the indirect method (single-point measurement) is able to main-

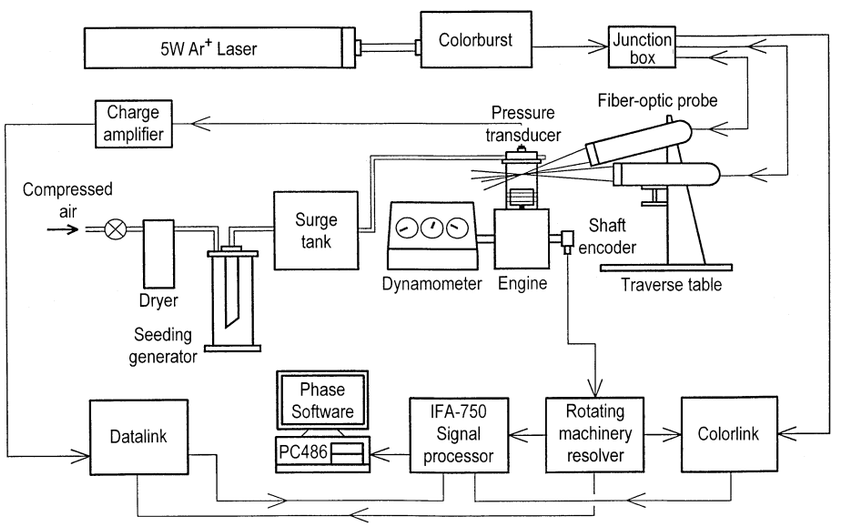

Fig. 1. Schematic diagram of the test rig configuration

Table 2. Specifications of the laser Doppler velocimeter system

LDV manufacturer	TSI	
Transmitting lens focal length	Blue:	499.5 mm
	Purple:	349.8 mm
Beam spacing	50 mm	
Beam diameter	2.1 mm	
Beam intersection half angle	Blue:	2.8°
	Purple:	3.9°
Number of fringes	Blue:	33.9
	Purple:	35.1
Fringe spacing	Blue:	4.88 μm
	Purple:	3.34 μm
Probe volume dimension	Blue:	165.5 μm × 3.4 mm
(diameter × length)	Purple:	117.2 μm × 1.7 mm
Effective frequency shift	+10 MHz	
Signal processor	Digital burst correlator TSI IFA 750	
Seeding particles	0.7 μm MgO	
Laser power source	Coherent Innova 90 5 W Ar^+ laser	

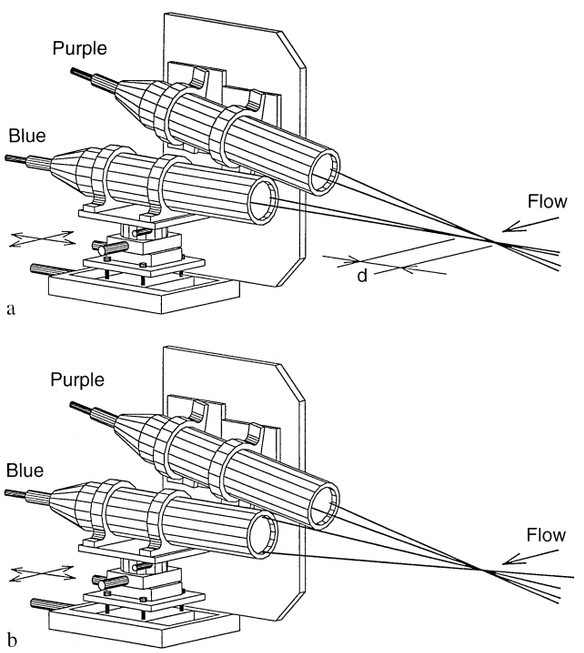

Fig. 2. Schematic of the traverse table for (**a**) two-probe two-point 1-component measurement, where d denotes the distance between two focused points; and (**b**) two-probe single-point 2-component measurement

tain 5 to 50 kHz with good seeding technique. Nevertheless, when applying the same technique to the direct method (simultaneous two-point measurement), the sampling rate drops to 500 to 1500 Hz immediately. The latter is only about $\frac{1}{10}$ to $\frac{1}{30}$ of the former. This is due to the choice of the coincidence window, which is defined to be 10 μs according to the minimum correlation time of the smallest eddies. That largely reduces the data sampling rate even the operating condition is

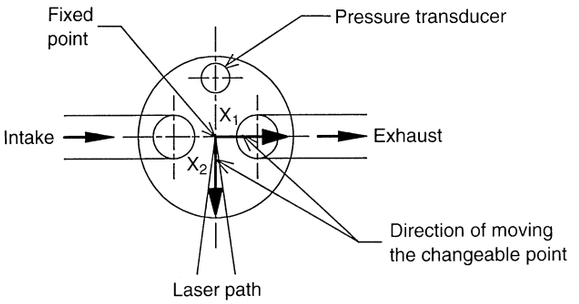

Fig. 3. Schematic diagram of the test section and the relative location of the fixed point and the changeable point

exactly the same. Another problem of the direct method used in this paper is the refraction correction for the optical path through the cylindrical boundary of the quartz liner. This is calibrated by optical alignment with cylinder head dismantled. The correction is also double-checked by calculations from the refraction formula derived by Vafidis (1985).

3
Data analysis

3.1
Length scale evaluated from indirect measurements

In a periodic nonstationary turbulent flow field, such as that inside the engine cylinder, the instantaneous velocity, U, measured from the LDV system can be decomposed into two components: an ensemble averaged mean velocity, U_{EA}, and a fluctuation velocity, u_F. In mathematical forms, their relation is

$$U(\bar{\theta}, i) = U_{\mathrm{EA}}(\bar{\theta}) + u_F(\bar{\theta}, i) \tag{1}$$

where

$$U_{\mathrm{EA}}(\bar{\theta}) = \frac{1}{N_t(\bar{\theta})} \sum_{i=1}^{N_c} U(\bar{\theta} \pm \Delta\theta/2, i) \tag{2}$$

In the above equations, $\bar{\theta}$ is the current crank angle position; i refers to the ith cycle; $\Delta\theta$ is the window width of crank angle $\bar{\theta}$; N_c is the total number of cycles; and N_t is the total number of measurements within crank angle window $\bar{\theta} \pm \Delta\theta/2$. The ensemble fluctuation intensity, $u'_{F,\mathrm{EA}}$, is defined by

$$u'_{F,\mathrm{EA}}(\bar{\theta}) = \left\{ \frac{1}{N_t(\bar{\theta})} \sum_{i=1}^{N_c} [U(\bar{\theta} \pm \Delta\theta/2, i) - U_{\mathrm{EA}}(\bar{\theta})]^2 \right\}^{1/2} \tag{3}$$

In order to separate the high frequency turbulence and low frequency cycle variation from each other, a low-pass-filtered cycle-resolved method (Liou and Satavicca, 1983) was employed. A new term, in-cycle bulk velocity, $\bar{U}(\bar{\theta}, i)$ was defined. The instantaneous velocity is again

$$U(\bar{\theta}, i) = \bar{U}(\bar{\theta}, i) + u_T(\bar{\theta}, i) \tag{4}$$

where u_T is the turbulence velocity. The in-cycle bulk velocity is a function of the crank angle and is different from cycle to cycle. Hence, the turbulence intensity decomposed from the

fluctuation intensity is defined to be

$$u'_{T,\mathrm{EA}}(\bar{\theta}) = \left\{ \frac{1}{N_t(\bar{\theta})} \sum_{i=1}^{N_c} [U(\bar{\theta} \pm \Delta\theta/2, i) - \bar{U}(\bar{\theta}, i)]^2 \right\}^{1/2} \quad (5)$$

and the root mean square of the cyclic variation is

$$\bar{U}_{\mathrm{RMS}}(\bar{\theta}) = \left\{ \frac{1}{N_c} \sum_{i=1}^{N_c} [U(\bar{\theta}, i) - \bar{U}_{\mathrm{EA}}(\bar{\theta})]^2 \right\}^{1/2} \quad (6)$$

where $\bar{U}_{\mathrm{EA}}$ is the ensemble average of the in-cycle bulk velocity using the same formula as Eq. (2). From turbulence textbooks (e.g.: Tennkes and Lumley 1972), an Eulerian temporal auto correlation coefficient, R_T, for the in-cylinder nonstationary flow version can be re-defined to be

$$R_T(\bar{\theta}, \phi) = \frac{1}{N_c} \frac{\sum_{i=1}^{N_c} u(\bar{\theta}, i) \cdot u(\bar{\theta} + \phi, i)}{u'_{\mathrm{EA}}(\bar{\theta}) \cdot u'_{\mathrm{EA}}(\bar{\theta} + \phi)} \quad (7)$$

where ϕ refers to the phase angle with respect to the crank angle $\bar{\theta}$; u and u'_{EA} are velocity and intensity respectively. The integral time scale, τ_I, is defined as the area below the curve of temporal autocorrelation coefficients with respect to the phase angle, i.e.,

$$\tau_I = \int_0^{\phi_{\max}} |R_T(\bar{\theta}, \phi)| \, d\phi \quad (8)$$

where $\phi_{\max}$ is the maximum phase angle that velocity fluctuation is no longer correlated. For flows without mean motion, the time scale indicates the lifetime of the large eddies; while for flows with mean motion, it means the eddy transit time.

To evaluate the integral length scale from the time scale using the indirect method, a Taylor's hypothesis (Hinze 1975) is normally employed. The hypothesis assumes that (i) the flow field is isotropic and homogeneous; (ii) the mean velocity in the flow field is stationary or quasi-steady; and (iii) the velocity fluctuation is very small compared with the mean velocity, then the integral length scale can be related with the time scale by

$$L_I(\bar{\theta}) = |U_{\mathrm{EA}}(\bar{\theta})| \cdot \tau_I(\bar{\theta}) \quad (9)$$

The length scale evaluated from this hypothesis is called "indirect length scale" in this paper.

3.2
Length scale evaluated from direct measurements

From the viewpoint of flow physics, the integral length scale is an indication of the size of eddies formed inside the turbulent flow, with the larger, energy containing eddies dominating the magnitude. To measure the in-cylinder integral length scale directly, simultaneous velocity measurements at two separated locations have to be conducted. The spatial correlation coefficients for the in-cylinder nonstationary turbulent flow field have to be defined first. According to the velocity fluctuation components that are collinear or parallel, as shown in Fig. 4, a lateral correlation coefficient, R_g, and a longitudinal correlation coefficient, R_f, are defined. In the similar form as Equation (7), they are expressed by

$$R_g = (\bar{\theta}, r_2) = \frac{1}{N_t - 1} \sum_{i=1}^{N_t} \frac{u_1(\bar{\theta}, x_2, i) \cdot u_1(\bar{\theta}, x_2 + r_2, i)}{u'_1(\bar{\theta}, x_2) \cdot u'_1(\bar{\theta}, x_2 + r_2)} \quad (10)$$

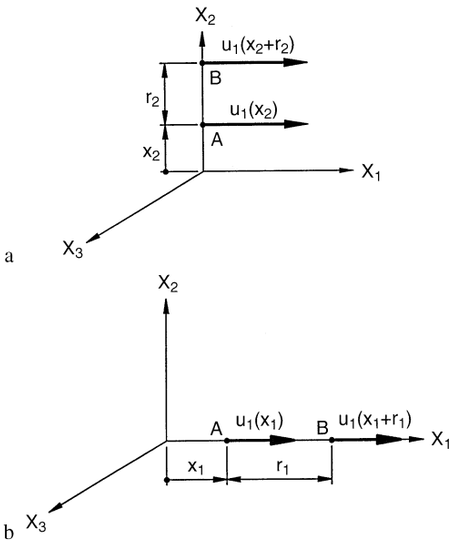

Fig. 4a, b. Schematic diagram of the spatial relation and direction of the velocity measurements for the lateral and longitudinal correlation coefficients

and

$$R_f = (\bar{\theta}, r_1) = \frac{1}{N_t - 1} \sum_{i=1}^{N_t} \frac{u_1(\bar{\theta}, x_1, i) \cdot u_1(\bar{\theta}, x_1 + r_1, i)}{u'_1(\bar{\theta}, x_1) \cdot u'_1(\bar{\theta}, x_1 + r_1)} \quad (11)$$

where x_1, x_2 are the fixed points on axes of X_1, X_2; r_1, r_2 are the distances between the changeable points and the fixed points on axes of X_1 and X_2; u_1 is velocity fluctuation in the direction of X_1 axis and u'_1 is its velocity fluctuation intensity.

The direct integral length scale is defined as the area below the curve of the spatial correlation coefficients with respect to the separation distance. The lateral integral length scale can be calculated by

$$L_g(\bar{\theta}, x_2) = \int_0^{r_2^*} R_g(\bar{\theta}, r_2) \, dr_2 \quad (12)$$

and the longitudinal integral length scale can be evaluated by

$$L_f(\bar{\theta}, x_1) = \int_0^{r_1^*} R_f(\bar{\theta}, r_1) \, dr_1 \quad (13)$$

where r_1^*, r_2^* are the distances between the changeable points and the fixed points that make $R_f(\bar{\theta}, r_1) = 0$, $R_g(\bar{\theta}, r_2) = 0$ at first time respectively. When $r_1 > r_1^*$ or $r_2 > r_2^*$, that means fluctuation velocity is no longer correlated.

3.3
Length scale evaluated from turbulence modelling

Using a simple k–ε turbulence sub-model, the turbulence dissipation length scale, L, can be calculated by the relation of the kinetic energy, k, and the viscous dissipation rate, ε, as follows;

$$L = \frac{c_\mu^{3/4} k^{3/2}}{\varepsilon} \quad (14)$$

where c_μ is an empirical constant of 0.09. If the turbulent flow is assumed to be isotropic, ε can be simplified to be a function of the turbulence intensity, u', and the Taylor's length scale, λ, i.e.,

$$\varepsilon = 15\nu \frac{u'^2}{\lambda^2} \tag{15}$$

where ν is the kinetic viscosity, which is equal to 15.37 $\mu m^2/s$ for air at 25 °C. The turbulence kinetic energy is defined by

$$k = \frac{3}{2} u'^2 \tag{16}$$

From the above equations, if the dissipation length scale is assumed to be approximate to the Taylor's length scale, then

$$\lambda = 15 \frac{\nu u'^2}{c_\mu^{3/4} k^{3/2}} = 49.7 \frac{\nu}{u'} \tag{17}$$

The Taylor's length scale can be related to the integral length scale with the following relation

$$\frac{\lambda}{L_I} = \left(\frac{15}{A}\right)^{1/2} \left(\frac{\nu}{u' L_I}\right)^{1/2} \tag{18}$$

where A is an undetermined constant, whose magnitude order is 1. Hence, the integral length scale is

$$L_I = \frac{A\lambda^2 u'}{15\nu} \approx 164.7 \frac{\nu}{u'} \tag{19}$$

Since u' is measurable in the experiment, the integral length scale can be estimated through this turbulence model.

4 Results and discussion

4.1 Comparison between ensemble and cycle resolved indirect length scales

Using the traditional single-point measurement technique, the indirect integral length scale can be obtained by both ensemble average and cycle resolved analyses as described in Sect. 3.1. Figure 5 shows the measurement results of the velocity component along the X_1 axis at the fixed point. If the data sampling rate is fast enough and the sampling size is large enough (40 kHz and 400 K samples or 250 cycles in this case), the ensemble averaged velocity and the ensemble average of the bulk velocity should be exactly the same, as shown in Fig. 5a. Fig. 5b indicates that the fluctuation intensity is the combination of the turbulence intensity and the root mean square fluctuation of the bulk velocity. The relation in mathematics is

$$u'_{F,\mathrm{EA}} = \sqrt{u'^2_{T,\mathrm{EA}} + \bar{U}^2_{\mathrm{RMS}}} \tag{20}$$

From the scale of the diagram, the magnitudes of the mean velocity and the turbulence intensity are in the same order. That implies the nonstationary flow field is dominated by the turbulence rather than the mean motion. In fact, that makes the Taylor's hypothesis not so applicable in this flow field. Hence, the indirect length scale calculated later can only be treated as a preliminary estimation.

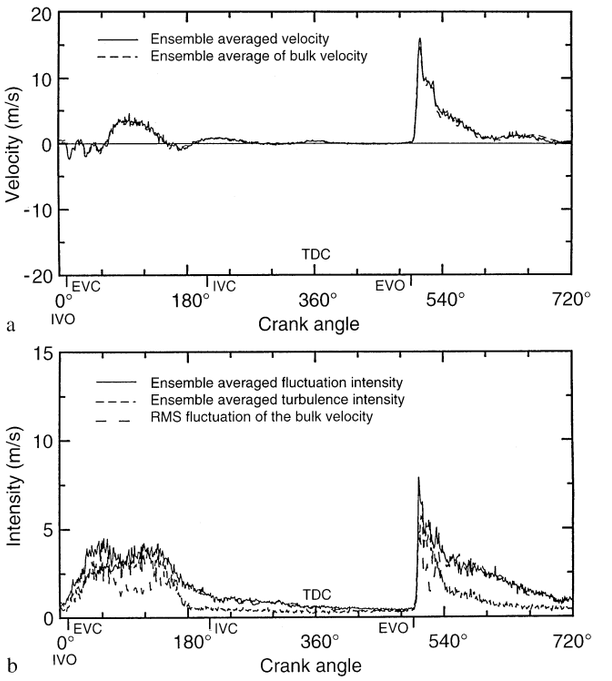

Fig. 5a, b. Measurement results of the mean velocity and intensities along the X_1 direction at the fixed point, which is located at the center of the plane 13 mm below the cylinder head

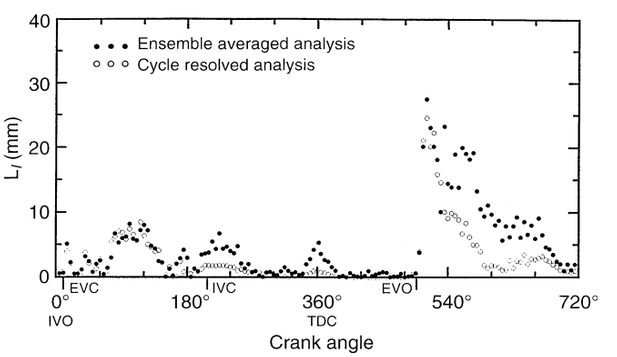

Fig. 6. Comparison of indirect length scales evaluated from ensemble averaged and cycle resolved analysis

Figure 6 shows the indirect integral length scales obtained from the ensemble average and the cycle resolved approach. This figure indicates that both length scales have the same trend with respect to the crank position, because basically they are all determined by the mean velocity and the time scale according to the hypothesis. The ensemble averaged length scale is larger than the cycle resolved one. This is because the former over-predicts the time scale. (The reason is that the ensemble average analysis mixed the low frequency cycle variation to the calculation of the fluctuation velocity.) That tends to increase the length scale estimation as well.

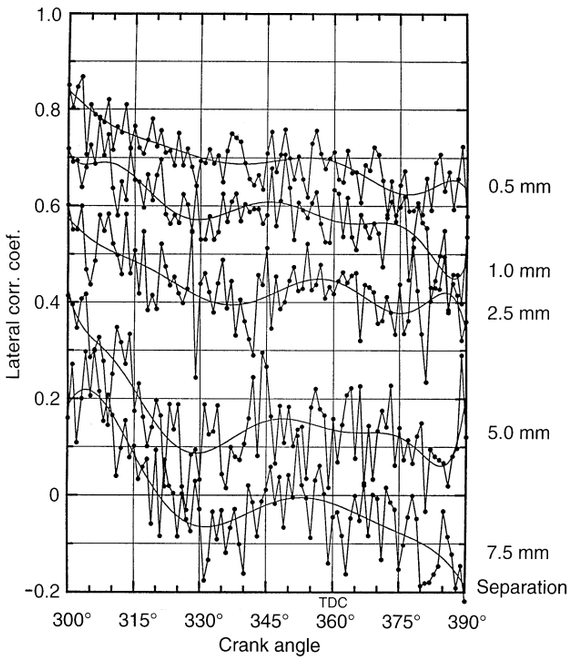

Fig. 7. Variation of lateral correlation coefficients with respect to the crank position and the separation distance

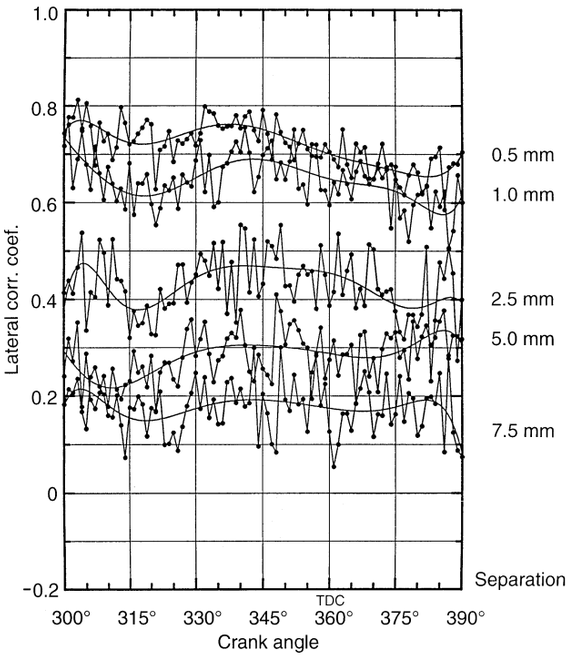

Fig. 8. Variation of longitudinal correlation coefficients with respect to the crank position and the separation distance

4.2
Comparison between longitudinal and lateral direct length scales

If we move the measurement location of the changeable point along the X_1 and X_2 axes, the variation of the spatial correlation coefficients for the whole cycle at each separation distance can be obtained. The lateral and longitudinal correlation coefficients calculated by Eqs. (10) and (11) are illustrated in Figs. 7 and 8. These two figures indicate that the coefficients decrease monotonously as the changeable point moves further away from the fixed point. However, the fluctuation is very serious. If an eighth order polynomial curve is fitted to those measurement points between crank angle 300–390°, we can plot the spatial correlation coefficients versus the separation distance as shown in Fig. 9. The magnitude of the integral length scale is then obtained by integrating the coefficient over the separation distance as described by Eqs. (12) and (13). Table 3 displays the comparison of the experimental results of

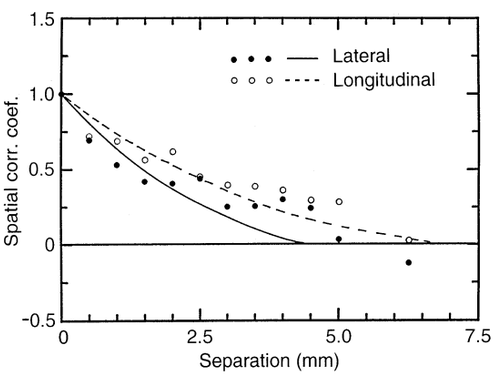

Fig. 9. Variation of lateral and longitudinal correlation coefficients with respect to the separation distance at the crank position 330 °CA

Table 3. Comparison of integral length scales of different engines at 30° BTDC measured by various LDV techniques

Technique	2-probe 2-point (present work)	2-probe-volume (Corcione, 1990)	Elongated volume (Fraser 1989)	Scanning LDV (Glover 1988)
Engine	Megatech MK3	Ruggerini RP170	Waukesha CFR	Ricardo Hydra
Bore (mm)	41	100	82.6	85.7
Stroke (mm)	51	95	114.3	86
Compression ratio	4	21	5.7	9
Motoring speed (rpm)	500	600	600	1200
Chamber shape	Pan-cake	Toroidal	Pan-cake	Pan-cake
Longitudinal (mm)	6.0	—	—	6.9
Lateral (mm)	3.9	2.2	3.1	3.4

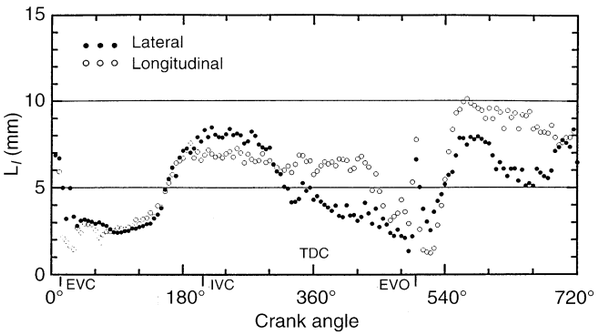

Fig. 10. Comparison of lateral and longitudinal direct integral length scales with respect to crank angle

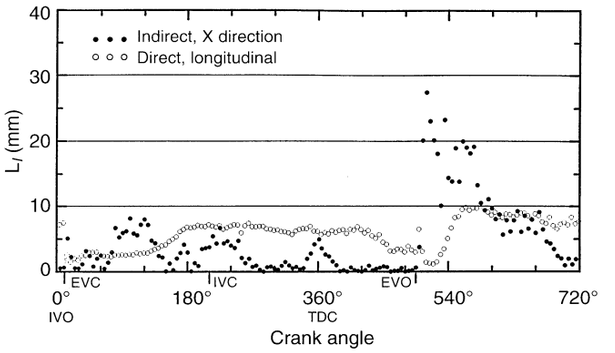

Fig. 11. Comparison of the longitudinal direct integral length scale with the indirect length scale along the X_1 aixs

the direct length scales at crank angle 330° with published results from various references using the similar LDV techniques. Although the engine and the operating conditions are a bit of difference, the length scales are in the same order. This gives an useful quantitative information to engine designers.

Using the above approach, the diagram of the direct integral length scales versus the crank angle can be illustrated in Fig. 10. From the variation of length scales in the whole cycle, it can be judged that the length scale is basically influenced by the inflow and outflow jet as well as the compression and expansion motion from the moving piston. At both top dead centers of 360° and 720°, the eddies expand their longitudinal and lateral length scales when the piston tends to compress the in-cylinder flow axially. The longitudinal length scale is larger than the lateral one near the TDC in the closed period. However, the magnitude of the former is not the twice of the latter. This result implies that the flow field in this particular engine exhibits inhomogeneity and anisotropy even when the piston is almost still and the turbulence kinetic energy has decayed almost completely.

4.3
Comparison between indirect and direct integral length scales

Figure 11 shows the comparison between the indirect length scale along the X_1 direction with the direct longitudinal length scale. These two scales show different tendency and magnitude. Since the direct length scale is measured directly and is regarded as the most accurate answer so far, the indirect length scale from the Taylor's hypothesis can only be treated as a preliminary guess. The indirect length scale under-estimates the length scale during the closed period, while over-predicts that during the open period. The only exception happens at the TDC, where both length scales are in reasonable agreement. This result is useful for quantitative estimation in practical applications to estimate the length scale using the simple indirect method.

4.4
Comparison between direct length scale and turbulence model estimation

Figure 12a shows that the estimated length scale from the k–ε sub-model tends to have different trend and magnitude with

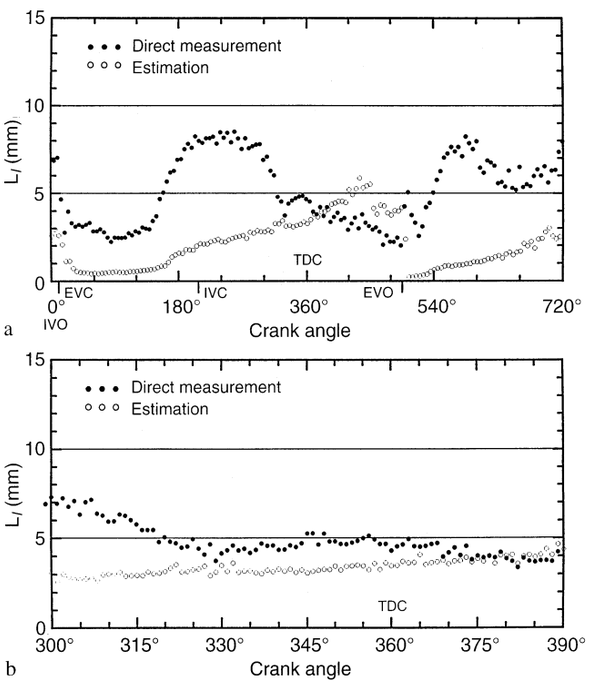

Fig. 12. **a** Comparison of the integral length scales estimated from the k–ε turbulence sub-model and the direct measurement; **b** is the enlarged view from 300° to 390 °CA

the direct length scale. However, if we enlarge the period between 330 and 390°, as shown in Fig. 12b, the two curves quite agree with each other. It implies that although the turbulent flow field is non-isotropic and inhomogeneous during this period, the degree of anisotropy and inhomogeneity doesn't invalidate the k–ε turbulence model. However, if this turbulence model wants to fit all the experimental results for the whole cycle, it has to be further improved.

5
Conclusions

1. Three approaches of obtaining in-cylinder integral length scales have been carefully studied. Among them, the two-probe

two-point LDV technique is referred as the direct measurement, which can be regarded as a fundamental and accurate method.

2. Comparing the results from indirect measurements and direct measurements, the indirect length scale shows wrong tendency as well as incorrect magnitude. This is because the Taylor's hypothesis is unsuitable to the in-cylinder nonstationary turbulent flow field.

3. From the comparison of the lateral and the longitudinal direct length scales, the magnitude of the longitudinal one is larger than, but not the twice of, the lateral one in the vicinity of TDC (330° in the example). That means the velocity field tends to, but still doesn't, reach homogeneous and isotropic condition, although the piston is almost still and the turbulence kinetic energy induced from the intake jet has decayed almost completely during then.

4. The estimate of the length scale from the k–ε sub-model shows reasonable agreement in both mangnitude and tendency, between crank angle 330°–390°. A preliminary conclusion can be reached that the k–ε turbulence sub-model is adequate to the in-cylinder turbulence modelling during this period for this particular engine. However, it still needs to be further improved.

5. The whole paper concludes that the two-probe two-point LDV measurement, described in this paper, is an adequate and accurate method when dealing with the investigation of in-cylinder length scales. The current traverse table can be slightly modified to measure the axially separated lateral and longitudinal length scales for future studies.

References

Corcione FE; Valentino G (1990) Turbulence length scale measurements by two-probe-volume LDA technique in a diesel engine. SAE Paper 902080

Fraser RA; Pack CJ; Santavicca DA (1986) An LDV system for turbulence length scale measurements. Exp Fluids 4: 150–152

Fraser RA; Felton PG; Bracco FV; Santavicca DA (1986) Preliminary turbulence length scale measurements in a motored IC engine. SAE Paper 860021

Fraser R; Bracco FV (1988) Cycle-resolved LDV integral length scale measurements in an IC Engine. SAE Paper 880381

Fraser RA; Bracco FV (1989) Cycle-resolved LDV integral length scale measurements investigating clearance height scaling, isotropy and homogeneity in a I.C. engine. SAE Paper 890615

Glover AR; Hundleby GE; Hadded O (1988) The development of scanning LDA for the measurement of turbulence in engines. SAE Paper 880378

Glover AR; Hundleby GE; Hadded O (1988) An investigation into turbulence in engines scanning LDA. SAE Paper 880379

Hinze JO (1975) *Turbulence*. 2nd ed. McGraw-Hill, New York

Ikegami M; Shioji M; Nishimoto K (1987) Turbulence intensity and spatial length scale during compression and expansion strokes in a four-cycle reciprocating engine. SAE Paper 870372

Liou TM; Santavicca DA (1983) Cycle resolved turbulence measurements in a ported engine with and without swirl. SAE Paper 830419

Liou TM; Santavicca DA (1985) Cycle resolved LDV measurements in a motored IC engine. Transaction of the ASME. J Fluid Engr 107: 232–240

Tennekes H; Lumley JL (1972) *A first course in turbulence*. The MIT Press Cambridge, MA

Vafidis C (1985) Aerodynamics of reciprocating engines. PhD Thesis, Imperial College. 94–97